Shahrekord University

Journal of Microfluidic and Nanofluidic Research

Journal homepage: https://jmnr.sku.ac.ir

JMNR

Research Article

Modeling Drop-Wall Interaction in the Film Boiling Regime under an Alternating-Current Electric Field

Reza Ghadami, Pedram Pournaderi *

Department of Mechanical Engineering, Yasouj University, Yasouj, Iran

ARTICLE INFO

Article history:
Received: 2025-07-01
Revised: 2025-08-05
Accepted: 2025-08-08

Keywords:
Electrohydrodynamics;
Collision;
Drop;
Film boiling regime;
Alternating current.

ABSTRACT

In this paper, the drop-wall interaction in the film boiling regime under an alternating-current electric field is simulated based on perfect dielectric theory. A sharp interface approach (combination of the level-set and ghost fluid method) is implemented to model the interface accurately. Subject to an alternating-current electric field, the spreading extent of the droplet is reduced. However, the electric stresses act in a way that the droplet height at the rebounding moment and contact time of the droplet on the surface increase. The obtained results prove that the influence of the voltage frequency on the spreading extent, droplet height and contact time is slight. According to the results, the total heat dissipated from the surface is enhanced under an alternating-current electric field, especially, at lower Weber numbers. At other Weber numbers, the effect of the voltage frequency is not remarkable. At the low Weber numbers, the most value of the dissipated heat is observed at the highest voltage frequency.

1. Introduction

During the impingement process of a droplet on a superheated surface, a thin vapor layer forms between the droplet and the surface. In this case, the direct contact between the droplet and surface does not occur and heat transfer rate decreases. This regime of impact is called film boiling or Leidenfrost regime. This phenomenon is observed in many practical applications such as spray cooling of heated surfaces and fuel injection in internal combustion engines. In recent years the use of electric fields has been developed as an effective approach for controlling the hydrodynamic and heat transfer of the fluid flows.

There are very limited investigations on the droplet collision with superheated surfaces under the effect of electric fields. Takano et al. [1] examined the influence of an applied electric field on the heat transfer of the sessile ethanol droplets and reported a remarkable increase in the evaporation rate. Celestini and Kirstetter [2] conducted an experiment to study the effect of the electric field on the sessile Leidenfrost droplets. They found that the vapor layer thickness decreases under an electric field. Wildeman and Sun [3] focused on the low energy impacts both experimentally and analytically and reported an increase in the bouncing height of the droplet subjected to an electric field. Shahriari et al. [4] carried out experiments on Leidenfrost sessile droplets and found beyond a specific voltage the Leidenfrost phenomenon is suppressed. Ozkan et al. [5] examined the Leidenfrost suppression phenomenon for sessile

* **Corresponding author.**
E-mail address: *sp.pournaderi@yu.ac.ir*

Cite this article as:

Ghadami, R. and Pournaderi, P., 2025. Modeling Drop-Wall Interaction in the Film Boiling Regime under an Alternating-Current Electric Field. *Journal of Microfluidic and Nanofluidic Research*, 2(3), pp. 151-156. https://doi.org/10.22034/jmnr.2026.15016.1002

droplets under AC electric fields and reported that by increasing the frequency the suppression of the vapor layer weakens. Nazari and Pournaderi [6] simulated the Leidenfrost impact of perfect conductive droplets subjected to a DC electric field and observed an enhancement in the droplet spreading radius, contact time and heat transfer rate. Lu et al. [7] focused on the suppression of the film boiling phenomenon under AC electric fields experimentally and found that maximum suppression occurs at certain frequencies. Ghadami and Pournaderi [8] simulated the impingement of both perfect and leaky dielectric droplets on a superheated substrate under a DC electric field. They observed an enhancement in the total heat dissipation from the wall for leaky dielectric droplets. However, no important change in the total heat removal was reported for the perfect dielectric droplets.

The literature review above, shows that the researchers often employed the experimental tools to investigate the hydro-thermal behavior of sessile droplets on superheated substrates subjected to electric fields. To the best of the authors knowledge, there are only two works [6, 8] that considers the droplet impact on superheated surface under electric fields numerically. However, both of these works focused on the impact process under DC electric field. In the present work, the effect of an alternating current electric field on the impingement process of a dielectric droplet on a heated surface in the film boiling regime is investigated numerically.

2. Basic Equations

2.1. Flow, Energy and Electrostatic Equations

The governing equations include the flow, energy, and electrostatic equations:

$$\nabla.\boldsymbol{u}=0 \tag{1}$$

$$\frac{\partial \boldsymbol{u}}{\partial t}+(\boldsymbol{u}.\nabla)\boldsymbol{u}=-\frac{1}{\rho}\nabla p+\frac{1}{\rho}\nabla.(\tau^H+\tau^E)+\boldsymbol{g} \tag{2}$$

where, hydrodynamic and electric stress tensors are calculated as:

$$\tau^H=\mu(\nabla\boldsymbol{u}+\nabla\boldsymbol{u}^T) \tag{3}$$

$$\tau^E=\epsilon(\boldsymbol{EE}-\frac{1}{2}\boldsymbol{E}.\boldsymbol{EI}) \tag{4}$$

ϵ , $\boldsymbol{E}$, and $\boldsymbol{I}$ show electrical permittivity, electric field vector and identity tensor, respectively.

The energy equation is used to calculate the temperature field:

$$\frac{\partial T}{\partial t}+(\boldsymbol{u}.\nabla)T=\frac{1}{\rho C_p}\nabla.(k\nabla T) \tag{5}$$

For a perfect dielectric medium, the following equation is used to calculated the electric potential :

$$\nabla.(\varepsilon\nabla\psi)=0 \tag{6}$$

After calculation of the electric potential, the electric field vector is calculated as $\boldsymbol{E}=-\nabla\psi$.

2.2. Interfacial Jump Conditions

In this paper, the jump in quantity A across the interface is shown as $[A]$. In vaporizing two-phase flows, applying mass conservation principle at the interface leads to the following jump condition for the velocity field [6, 8]:

$$[\mathrm{u}]=\dot{m}[\frac{1}{\rho}]\boldsymbol{n} \tag{7}$$

$\boldsymbol{n}$ and $\dot{m}$ shows unit normal vector at the interface and vaporization rate per unit surface, respectively.

By applying the momentum principle at the interface, the following jump conditions for pressure and viscous terms are derived [6, 8]:

$$[p]-2[\mu]\boldsymbol{n}.\nabla\boldsymbol{u}\cdot\boldsymbol{n}^T-\boldsymbol{n}\cdot[\varepsilon\left(\boldsymbol{EE}-\tfrac{1}{2}\boldsymbol{E}.\boldsymbol{EI}\right)]\cdot\boldsymbol{n}^T=\gamma\kappa-\dot{m}(\tfrac{1}{\rho}) \tag{8}$$

$$[\mu\nabla\boldsymbol{u}]=[\mu](\nabla\boldsymbol{u})\binom{\boldsymbol{0}}{\boldsymbol{t}}^T\binom{\boldsymbol{n}}{\boldsymbol{t}}+[\mu]\boldsymbol{n}^T\boldsymbol{n}(\nabla\boldsymbol{u})\boldsymbol{n}^T\boldsymbol{n}-\binom{\boldsymbol{0}}{\boldsymbol{t}}^T\binom{\boldsymbol{0}}{\boldsymbol{t}}\left([\mu](\nabla\boldsymbol{u}^T)+\left[\varepsilon\left(\boldsymbol{EE}-\tfrac{1}{2}\boldsymbol{E}.\boldsymbol{EI}\right)\right]\right)\boldsymbol{n}^T\boldsymbol{n} \tag{9}$$

where $\boldsymbol{t}$, κ, and γ represent unit tangent vector, curvature, and surface tension, respectively. By applying energy equation at the interface, the following jump condition is obtained [6, 8]:

$$h_{lg}\dot{m}-[k\nabla T.\boldsymbol{n}]=0 \tag{10}$$

h_{lg} stands for the latent heat of evaporation.

For a perfect dielectric liquid, the electrostatic jump conditions across the interface are expressed as [6, 8]:

$$[\psi]=0 \tag{11}$$

$$[\varepsilon\nabla\psi.\boldsymbol{n}]=0 \tag{12}$$

3. Numerical Methods

The governing equations are solved based on the finite volume approach. The projection method [9] is adopted to solve the flow equations. The level set method along with the ghost fluid method [9, 10] are implemented to capture the interface accurately. The WENO [9] and central

approximation are used to discritize convection and diffusion terms, respectively. Also, the 3rd order TVD Runge-Kutta scheme [9] is used for temporal discretization.

3.1. Level-set Method

The level set method is used to determine the interface location. In this method, the level set function φ is defined as a signed distance function from the interface. Therefore, this function is zero at the interface, positive in one phase and negative in another phase. The governing equation of the level set function is expressed as [11-13]:

$$\frac{\partial \varphi}{\partial t} + \boldsymbol{u}_{int}.\nabla\varphi = 0 \quad (13)$$

where $\boldsymbol{u}_{int}$ is the interface velocity. The distance function property of the level set function ($|\nabla\varphi| = 1$) usually is lost during the solution. Therefore, the reinitialization equation should be solved:

$$\frac{\partial \varphi}{\partial \tau} = S(\varphi_0)(1 - |\nabla\varphi|) \quad (14)$$

τ , φ_0, and $S(\varphi_0)$ represent pseudo time, φ before reinitialization, and sign function, respectively.

3.2. Ghost Fluid Method

In this paper, the interfacial jump conditions are imposed using the ghost fluid method [9,10]. In two-phase flows, some quantities are discontinuous across the interface. In the ghost fluid method, by defining the ghost cells, each phase is extended into another phase. The values of the discontinuous quantity at the ghost cells are obtained based on the relevant jump conditions. Therefore, the derivatives of discontinuous quantities at the interface are calculated using the ghost cell values. More details can be found in [9, 10].

4. Results and Discussion

Figure 1 describes the collision problem of a saturated Hexane droplet on a superheated surface schematically. D_0 and V_0 are initial droplet diameter and velocity, respectively. The initial droplet diameter is considered to be 2.3 mm and the domain size is set to 5mm×12mm. The superheat temperature (the difference between the temperature of the wall and droplet) is 300^0C. Due to the symmetry of the problem, the equations are solved on the half of the domain. The no slip and Neumann conditions are applied on the bottom and left boundaries, respectively. On the other boundaries, free boundary condition is imposed. Under AC electric field, the applied electric potential on the upper boundary varies over the time as $V(t)=V_o\cos(2\pi f t)$. In this equation, V_0 and f are the amplitude of the electric potential and current frequency, respectively. The effective electric potential is expressed as $V_{RMS} = V_0/\sqrt{2}$. In this problem, the important dimensionless parameters are Weber ($We = \rho V_0^2 D_0/\gamma$) and electric capillary ($Ca_E = \varepsilon_e E^2 R_0/\gamma$) numbers. The electric field strength, E, is calculated based on the effective electric potential. Recently, we studied the effect of a DC electric field on the droplet impact on a superheated surface [8]. In our previous work, we validated our code by comparing the numerical results with an experiment [1]. Also, we showed that a mesh with a resolution of ($R_0/\Delta x = 34$) is sufficient to obtain accurate results.

Figure 2 shows the different stage of the impact process at We=15, $Ca_E = 5.09$, f=10kHz. The droplet spreads over the surface due to its inertia. The viscous and surface tension forces resist the droplet spreading. Once the maximum spreading radius is obtained the retraction process starts under the effect of the surface tension force. At the end of the retraction stage, the droplet rebounds from the surface due to its inertia. Throughout this process, due to the thin vapor layer between the droplet and the surface, the droplet does not touch the surface. As it is observed, since an AC electric field is applied the electric potential on the top boundary and as a result the direction of the electric field varies over the time.

Figure 3 depicts the electric field effect on the droplet spreading radius at different Weber numbers. As the Weber number increases the enhancement of the inertia force compared to the surface tension force leads to the enhancement of the droplet spreading radius. Under the applied electric field (DC or AC), the spreading radius decreases. Because the electric stresses act in the direction of the electric field and therefore resist

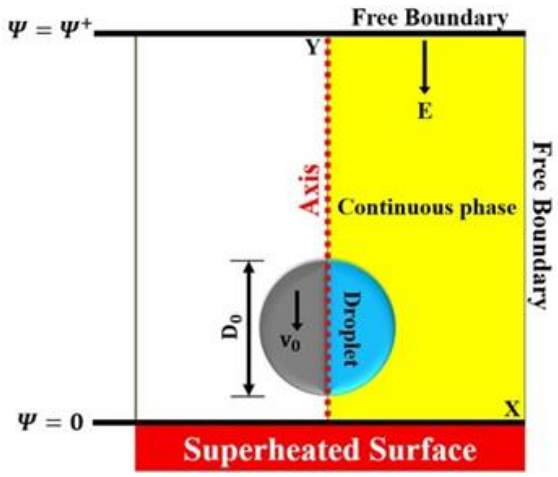

Fig. 1. Computational domain

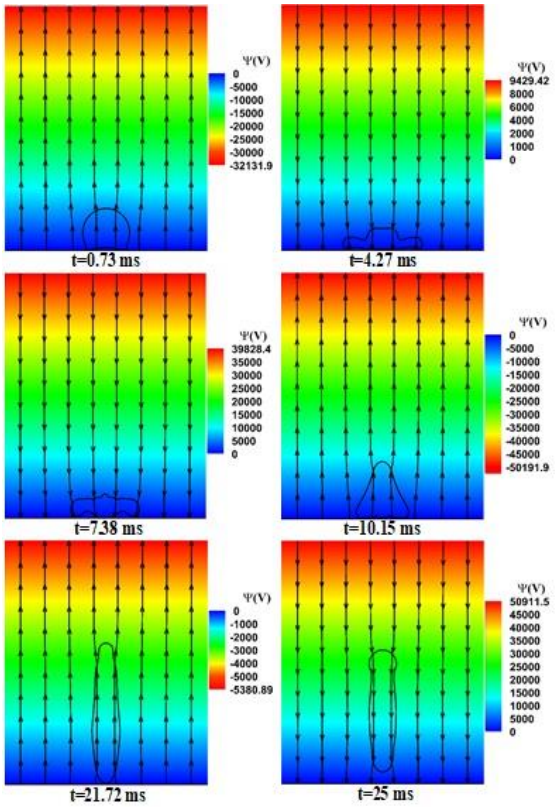

Fig. 2. Electric potential distribution and electric current lines during the impact process ($We = 15, Ca_E = 5.09, f = 10kHz$)

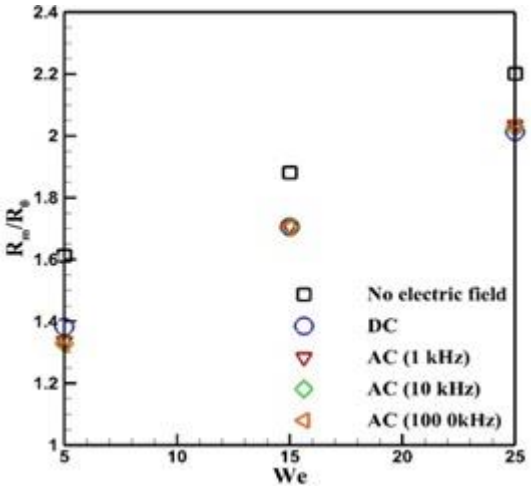

Fig. 3. Variations of droplet spreading radius versus Weber number under different electric fields

the droplet spreading. The droplet spreading radius for DC and AC electric fields is almost the same and the voltage frequency has no important effect on this parameter.

Figure 4 depicts the electric field effect on the droplet contact time at different Weber numbers. In the absence of the electric field, the Weber number has no important effect on the droplet contact time. However, under the applied electric field the contact time decreases.

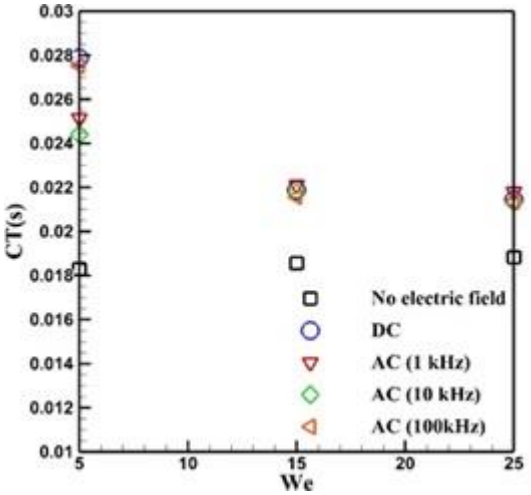

Fig. 4. Variations of droplet contact time versus Weber number under different electric fields

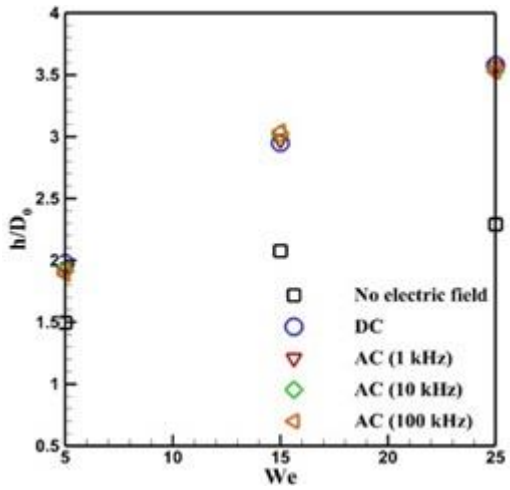

Fig. 5. Variations of droplet height at rebounding moment versus Weber number under different electric fields

According to the figure, the droplet contact time increases under an electric field. In other words, the normal electric stresses at the interface postpones the droplet rebounding form the surface. At higher Weber numbers, the type of the electric field (DC or AC) and the voltage frequency have no significant influence on the contact time. However, at the lower Weber number (We=5), under an AC electric field the droplet leaves the surface faster.

Figure 5 depicts the electric field effect on the droplet height at the rebounding moment at different Weber numbers. According to figure 5, the droplet height at the rebounding moment increases with Weber number. Also, the normal electric stresses at the interface elongates the droplet in the direction of the electric field and, therefore, the droplet height increases under an applied electric field. It can also be concluded that the type of the electric field (DC and AC) and the

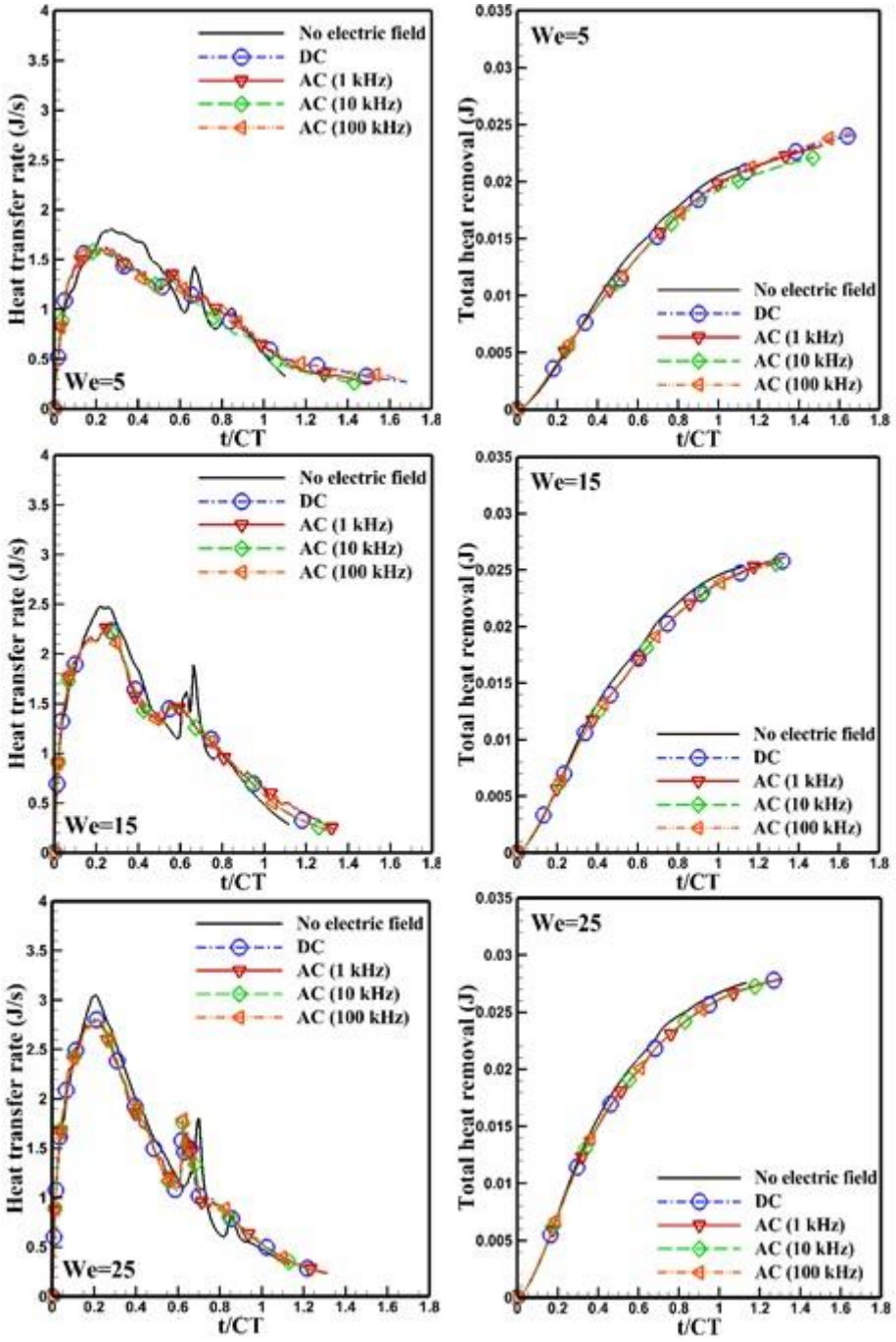

Fig. 6. Heat transfer rate and total heat removal from the surface

voltage frequency has no significant effect on the droplet height. Figure 6 shows the variations of heat transfer rate and total heat removal over the time. By increasing the Weber number and equivalently the inertia force, the vapor layer thickness decreases. Therefore, the heat transfer rate and total heat removal from the surface increases. When the electric field is applied the heat transfer rate decreases. This can be attributed to the enhancement of the vapor layer thickness under the effect of the normal electric stresses. However, the influence of the type of the electric field and voltage frequency is negligible. It can also be concluded that the total heat removal from the surface at the end of the impact process increases by applying an electric field. This increase is more remarkable at lower Weber numbers. Although by applying an electric field the heat transfer rate decreases the enhancement of the droplet contact time leads to the enhancement of the total heat removal at the end of the impact process. At the moderate and high Weber numbers, the influence of the electric field type and voltage frequency is very slight.

However, at the low Weber numbers, the most amount of the heat removal is related to case of the DC electric field and AC electric field with the highest frequency.

5. Conclusions

In this paper, the impingement of a perfect dielectric droplet on a superheated surface under an AC electric field is simulated. The level set method along with the ghost fluid method is used to model the interface accurately. The main results of this research are summarized as:

1- The droplet spreading radius, the droplet height at the rebounding moment, and the total heat removal from the surface increases with Weber number. But the droplet contact time decreases as the Weber number increases.

2- The type of the electric field (DC or AC) has no significant effect on the spreading radius, droplet height at the rebounding moment. Also, the effect of the electric field type on the contact time at moderate and high Weber numbers is negligible.

3- At the moderate and high Weber numbers, the influence of the electric field type on the total heat removal is very slight. However, at the low Weber numbers, the total heat removal for the DC electric field is higher.

4- Under an applied AC electric field, the droplet spreading radius decreases. However, the droplet contact time and droplet height at the rebounding moment increases. According to the results, the voltage frequency has no important effect on spreading radius, contact time and droplet height at the rebounding moment.

5- The total heat removal from the surface at the end of the impact process increases by applying an AC electric field. This increase is more remarkable at lower Weber numbers. At moderate and high Weber numbers, the influence of the voltage frequency is very slight. However, at the low Weber numbers, the most amount of the heat removal is related to the AC electric field with the highest frequency.

References

[1] Takano, K., Tanasawa, I., and Nishio, S., 1994. Active enhancement of evaporation of a liquid drop on a hot solid surface using a static electric field. International Journal of Heat and Mass Transfer, 37, pp. 65-71.

[2] Celestini, F., and Kirstetter, G., 2012. Effect of an electric field on a Leidenfrost droplet. Soft Matter, 8, pp. 5992-5995.

[3] Wildeman, S., and Sun, C., 2016. Electric field makes Leidenfrost droplets take a leap. Soft Matter, 12, pp. 9622-9632.

[4] Shahriari, A., Das, S., Bahadur, V., and Bonnecaze, R. T., 2017. Analysis of the instability underlying electrostatic suppression of the Leidenfrost state. Physical Review Fluids, 2, p.034001.

[5] Ozkan, O., Shariari, A., and Bahadur, V., 2017. Electrostatic suppression of the Leidenfrost state using AC electric fields. Applied Physics Letters, 111, p.141608.

[6] Nazari, H., and Pournaderi, P., 2019. The electric field effect on the droplet collision with a heated surface in the Leidenfrost regime. Acta Mechanica, 230, pp. 787-804.

[7] Lu, Y., Bao, J., and Liu, D., 2021. An experimental and theoretical investigation of electrostatic suppression of the Leidenfrost state. International Journal of Heat and Mass Transfer, 170, p.121036.

[8] Ghadami, R., and Pournaderi, P., 2024. Numerical study of droplet impact on a superheated surface under an electric field based on perfect and leaky dielectric theories. Heat Transfer, 53, pp. 3579-3604.

[9] Kang, M., Fedkiw R. P., and Liu, X. D., 2000. A boundary condition capturing method for multiphase incompressible flow. Journal of Scientific Computing, 15, pp. 323-360.

[10] Liu, X. D., Fedkiw R. P., and Kang, M., 2000. A boundary condition capturing method for Poisson's equation on irregular domains. Journal of computational Physics, 160, pp. 151-178.

[11] Yang, D., Sun H., Li, M., Li, Q., Gao, X., Chen, C., and He, L., 2023. Effect of electric field strength and droplet diameter on droplet–interface coalescence mechanism. Chemical Engineering Science, 282, p.119360.

[12] Lanjewar, S., and Ramji, S., 2024. Dynamics of a deformable compound droplet under pulsatile flow. Physics of Fluids, 36, p.083301.

[13] Pournaderi, P., and Pishevar, A. R., 2012. A numerical investigation of droplet impact on a heated wall in the film boiling regime. Heat and Mass Transfer, 48, pp. 1525-1538.